Computational Modeling and Deep Learning-Assisted Optimization of Composite Spinodal Topologies

Saltuk Yildiz+, Zekeriya Ender Eger++, Pinar Acar*

Virginia Tech, Blacksburg, 24061
VA, USA

saltuk@vt.edu

endereger@vt.edu

pacar@vt.edu

ABSTRACT

Spinodal metamaterials (spinodoids) exhibit enhanced mechanical properties due to their unique design, which allows for a wide range of smooth shapes. These geometries eliminate the high-stress concentrations and symmetry-breaking defects typically found in lattice structures with sharp features. As lightweight and next-generation structural architectures, spinodoids offer extraordinary mechanical performance, making them highly promising for applications in aerospace, automotive, and biomedical fields.

In this study, carbon fiber-reinforced polymer (CFRP) spinodoids are explored to optimize their mechanical performance. An analytical model is first developed to randomly generate spinodal geometries. Next, linear elastic finite element analyses (FEA) are conducted to assess the elemental energy fraction values related to stress/strain distributions. By developing a deep learning framework, which is found to be efficient in replacing the FEA, the spinodal material design that minimizes elemental energy fractions is identified. Finally, the mechanical performance of this optimized spinodal architecture is compared to that of traditional strut-based composite structures made from the same materials.

1.0 INTRODUCTION

Spinodal topologies exhibit remarkable mechanical performance owing to their wavy design features and effectively mimic complex systems in nature, offering distinct advantages for use as mechanical structures in engineering applications [1]. Spinodal topologies feature smoothly interconnected design elements that mitigate stress concentrations. These continuous architectures are primarily inspired by the phase separation behavior of materials, as described by the Cahn–Hilliard theory [2]. Forward and inverse design of spinodal topologies is attracting increasing attention from researchers due to their exceptional potential for high mechanical performance.

Kumar et al. [1] carried out the inverse design framework for functionally graded spinodal topologies, mimicking natural bone shapes. They proposed a data-driven design framework that predicts specific anisotropic stiffness values to meet desired mechanical performance criteria. Zheng et al. [3] introduced a surrogate model based on a deep neural network to determine the homogenized material properties of spinodal topologies, enabling the solution of a multi-scale topology optimization problem. Golnary and Asghari [4] have achieved the linkage between anisotropic mechanical features and spinodal topology designs using unsupervised machine learning. In a recent study, Liu and Acar [5] extracted 2D spinodal shapes providing desired homogenized properties by utilizing an inverse modeling approach through convolutional generative adversarial networks (CGAN).

These aforementioned studies have explored the potential of spinodal topologies as porous structures involving a two-phase architecture with solid and void inclusions. In the presented design framework, spinodal topologies are treated as two-phase composite structures, where the void regions of equivalent porous designs are modeled as a secondary material phase. Despite their potential, the mechanical performance of spinodal topologies composed of two-phase materials remains underexplored. One such example performance criterion relates to the energy fraction values under deformation. In the spinodal topology optimization framework, the energy fraction, which is the unit elastic strain energy stored by the structure, is selected as an objective to be minimized for improved overall stiffness. This mechanical performance metric is significant to evaluate and optimize the two-phase spinodoid, which has unique design features. Moreover, conventional numerical methods combined with finite element analysis (FEA) incur significant computational costs. To address these challenges, this study proposes an effective and computationally efficient deep learning-assisted optimization approach for composite spinodal topologies, aiming to minimize elemental energy fractions and thereby enhance stiffness and reduce high-stress/strain regions.

2.0 METHODOLOGY

In this section, computational designs, deep-learning-assisted and numerical design optimization frameworks for two-phase spinodal topologies are explained in detail.

2.1 Design of Spinodal Topologies

Spinodal metamaterials exhibit smooth topologies that mitigate stress concentrations and satisfy common manufacturing constraints. Recent advancements in design and fabrication techniques, particularly through 3D printing, have enabled the successful realization of these complex architectures. In this study, we focus on the numerical analysis and design optimization of 2D spinodal architectures composed of a two-phase carbon fiber-reinforced polymer (CFRP) composite, which can be 3D-printable through the fused filament fabrication (FFF) technique. The material model is adopted from the literature [7], where the longitudinal elastic moduli of the carbon fiber-matrix and pure nylon matrix phases are experimentally determined. First, spinodoids are numerically characterized as two-colored images, as shown in Figure 1 by following the Gaussian Random Field-based formulation [1-4] to identify two material phases. The resulting phases of the spinodoid are determined according to:

$$X(x) = \begin{cases} 1\ (fibers) & if\ \psi(x) \leq \phi_0 \\ 0\ (matrix) & else \end{cases} \qquad (1)$$

In Eq. [1], *X(x)* stands for presence of the fibers materials decides phases according to threshold value (ϕ_0) which is selected as 0.35.
The spinodal topologies are generated using spinodal decomposition that decides the phases utilizing the Gaussian Random Fields (GRFs). The phase function theoretically determines both phases of a spinodal topology as given in Eq. [2].

$$\psi(x) = \sqrt{\frac{2}{N}} \sum_{n=1}^{N} \cos\left(\beta \boldsymbol{\eta_n} \cdot \boldsymbol{x} + \gamma_n\right) \qquad (2)$$

According to the Eq. [2], these phases are defined by N number of cosine waves, non-zero constant (β), orientation distributions (η_n) (defined in Eq. [3]), and the phase angle (γ_n).

$$\boldsymbol{\eta_n} \sim U(\{\boldsymbol{k} \in S: (|\boldsymbol{k} \cdot \boldsymbol{e_1}| > \cos(\theta_1)) \oplus (|\boldsymbol{k} \cdot \boldsymbol{e_2}| > \cos(\theta_2)) \qquad (3)$$

In Eq. [3], S defines the unit circle, and the orientations are sampled from this unit circle in all possible directions with unit magnitudes. Here, $\boldsymbol{e_1}$ and $\boldsymbol{e_2}$ represent Cartesian basis and θ_1 and θ_2 are cone angles, where the cones are centered around the Cartesian basis. These independent cone angles in two planar directions determine the geometric anisotropy. According to Eq. [3], the random orientation distributions decide the resulting topology. In the presented design framework, cone angles are set as 15 and 90 degrees to ensure continuous design of phases. Moreover, N and β are selected as 3 and 6π, respectively. The volume fraction of the fiber-matrix material for each configuration is selected as 60%. The orientation distributions are characterized by 6 parameters in total, which serve as the design variables in the optimization framework described in Section 2.3.

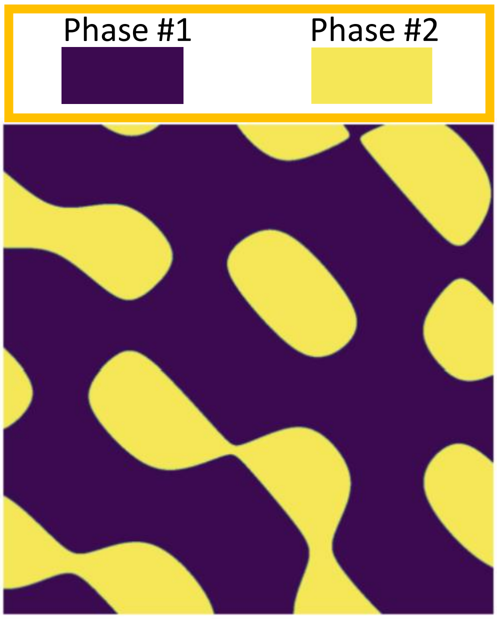

Figure 1: Example representation of a two-phase spinodoid geometry. Phase-1 (fiber-matrix) and Phase-2 (pure matrix) are assumed to hold different material properties.

The mechanical properties of the spinodoids depend on both the material properties of the constituent phases and the unique structural topology of the spinodoid. To compute the mechanical properties, the spinodal geometries are modeled using shell elements, and the three-node plane stress element (CPS3) is used for the FEA simulations. In this work, a linear elastic FEA is conducted using the ABAQUS/Standard software macro.

2.2 Finite Element Model

Spinodoids are numerically simulated under complex loading (shear and tension), and the unit cells are considered as having a fixed boundary condition as demonstrated in Figure 2. The tensile and shear loads are applied through a displacement equal to 20% of the domain length, which corresponds to 5000×5000 microns[2] (5×5 mm[2]), with each pixel representing 1 micron. The boundary conditions and meshing of two-phase spinodal topologies are defined in the FEA. A Delaunay-based mesh generation algorithm [6] is used to create the FEA mesh, which enables to generate mesh on black (fiber-matrix) and gray (pure matrix) regions. Total number of elements and nodes in the FEA setup are 145,500 and 80,300 in each design, respectively.

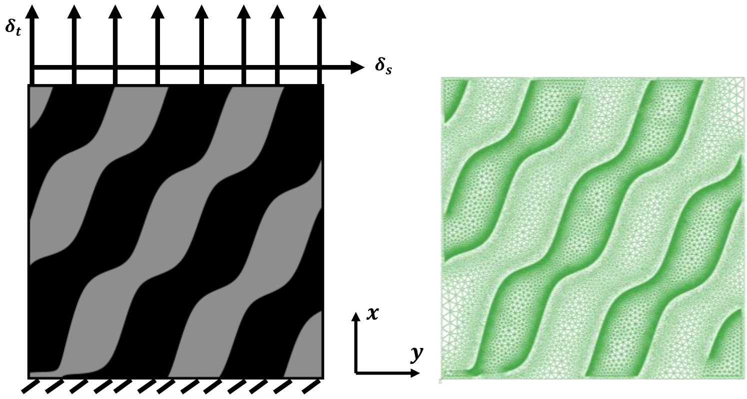

Figure 2 : Definition of the structural architecture, the boundary conditions and mesh details used in the FEA simulations. The black phase shows the fiber-matrix, and the gray phase shows the pure matrix.

The material properties of CFRP defined in FEA simulations for two-phase spinodal topologies are obtained from experimental tensile testing [7]. In material definition of the model, the fiber-matrix phase is assumed to be made of a carbon material with a very low amount of nylon and the polymer matrix is defined to be a pure nylon material.

Table 1: Material properties of a 3D Printed CFRP [7].

Elastic Property	Carbon	Nylon
Young's Modulus (GPa)	85	0.38
Poisson's Ratio	0.3	0.35

In numerical simulations, the strain energy density (W) is calculated for each design (see Eq. [4]). As shown in Eq. [5], this mechanical feature is summed for each element (i.e., M number of elements) to determine the total strain energy density (W_T) and the elemental energy fractions are derived through the ratio of strain energy density to the total strain energy density as given in Eq. [6].

$$W = \frac{1}{2}\sum_{i=1}^{2}\sum_{j=1}^{2}\sigma_{ij}\cdot\epsilon_{ij} \quad (4)$$

$$W_T = \sum_{k=1}^{M} W \quad (5)$$

$$E_f = \frac{W}{W_T} \quad (6)$$

2.3 Conventional and Deep-learning-assisted Optimization

A database of CFRP spinodoids is developed to train a deep learning model, which aims to replace the computationally expensive FEA simulations. The deep learning model involves a feed-forward neural network architecture (see Figure 3) that predicts the maximum and average elemental energy fraction values for two-phase spinodal designs as a function of numerical shape descriptors defining their smooth topologies. The optimization problem aims to solve for the optimum CFRP spinodoid topology minimizing the maximum and average elemental energy fraction values, which is a direct function of the maximum stress/strain concentration under loading.

The optimization results obtained using the deep learning-based surrogate model are compared with the results of the optimization framework using FEA simulations. Since the objective function is highly non-linear, a pattern search algorithm [8], a gradient-free optimization method, is employed. Moreover, the performance of the optimum spinodal configuration is compared with traditional strut-based lattice structures to demonstrate the effectiveness of spinodal architectures in mitigating stress/strain concentrations. The outcomes are expected to reveal more about the potential use of spinodoids in military applications, where low-density and high-strength are desired.

The baseline (initial) design is chosen based on uniformly distributed orientations, with spinodal features aligned at 45 degrees, resulting in a non-wavy structure as shown in Figure 4. The average energy fraction of this baseline model serves as a reference threshold for evaluating other configurations.

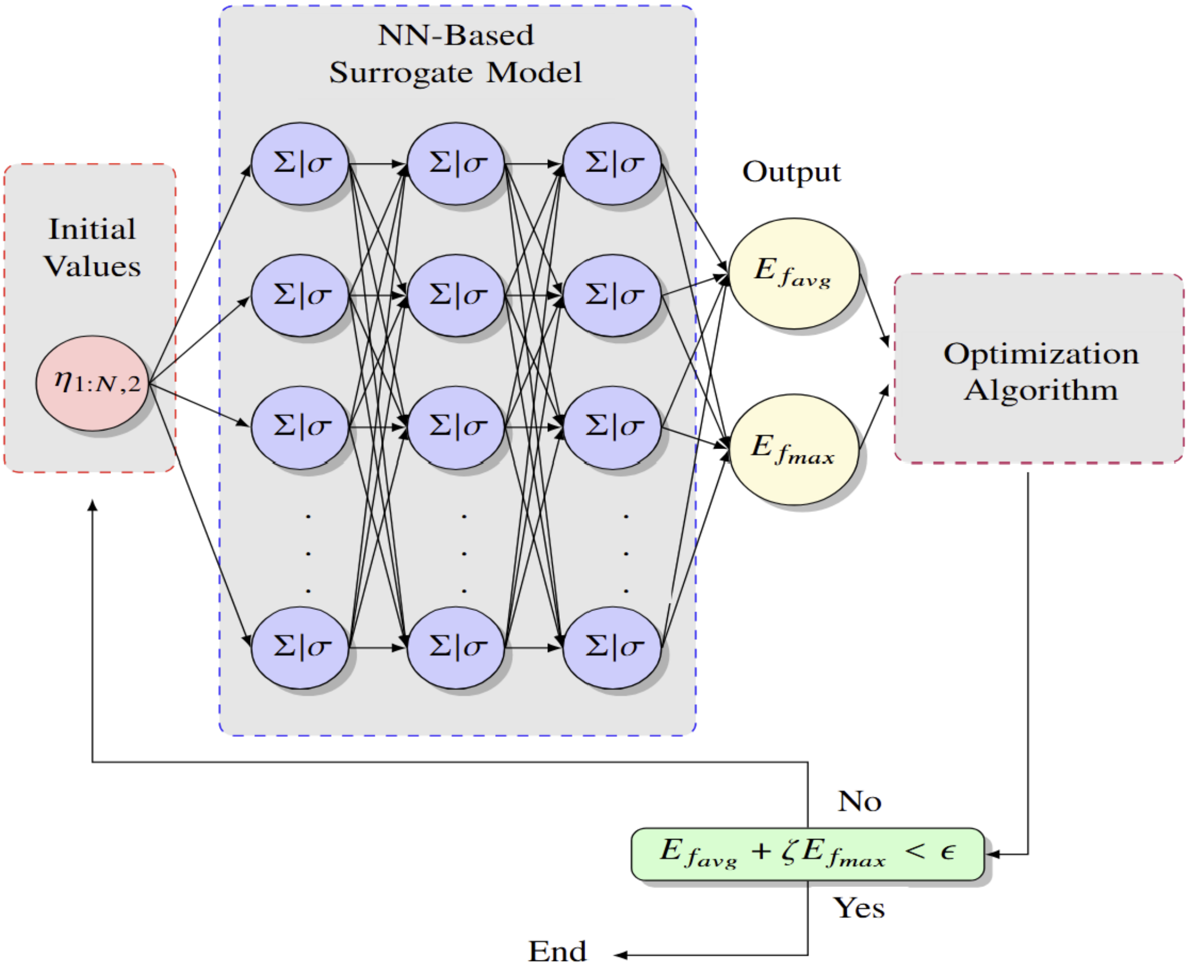

Figure 3 : A deep learning architecture to develop a surrogate model predicting the maximum and average elemental energy fractions as a function of the geometric descriptors of the spinodoids.

Figure 4 : Baseline (initial) spinodal material design.

The optimization formulation including the objective function, design parameters and constraints are given as below:

$$Minimize: avg(E_f) + \zeta \max(E_f)$$

$$Find: \eta_n \quad (7)$$

$$Subject\ to: \theta_1\ \&\ \theta_2$$

The objective function is defined as the minimization of both the average and maximum energy fraction values to reduce the stress/strain concentrations over a threshold. Here, the weight ζ is chosen as 0.5 to balance the relative magnitudes of the two objectives, ensuring that both are of the equivalent order of magnitude. In the data-driven framework, 400 data points are obtained through FEA, and 300 data samples are used for training, where the rest of the data samples are shared by validation and testing. The data generation takes approximately 31 hours on a cluster using an AMD EPYC 7702 CPU at 3.35 GHz.
In the feedforward neural networks, 128 neurons are used in a total of 3-layer, ReLU activation, and a 10% dropout is used. Larger configurations yield no notable improvement in accuracy while decreasing the layer size results in longer training times. Utilizing a compact feature set with 6 inputs and 2 outputs allows the training to complete within seconds. Given the significant variability in the maximum output values, log scaling is employed alongside normalization. The model demonstrates consistent performance across validation and test sets, achieving a mean absolute error (MAE) of 9.47%. While the conventional numerical optimization requires approximately one week to reach the optimal solution, the deep learning-assisted approach converges within minutes, resulting in a drastic reduction in computational time.

3.0 RESULTS AND DISCUSSIONS

The optimum design obtained with the surrogate-model-based framework of Section 2.3 is compared with the conventional optimization (i.e., pattern search method) result using FEA simulations in Figure 5.

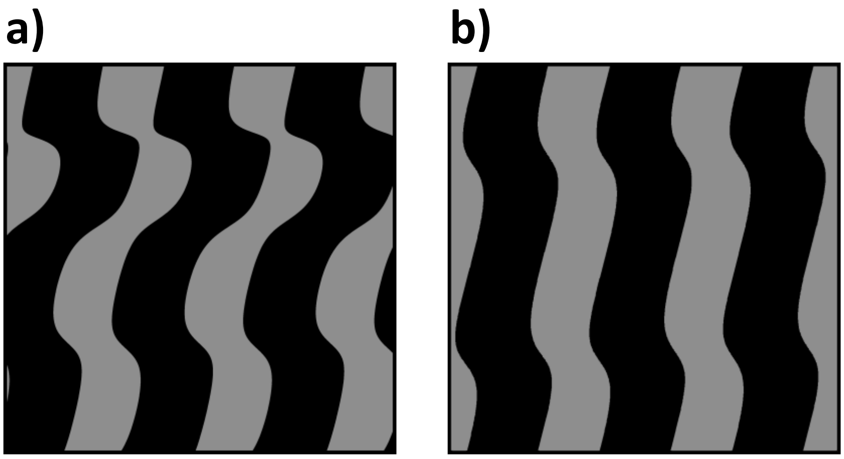

Figure 5 : Optimum spinodal topologies obtained using the a) surrogate-model, b) FEA.

The optimum spinodal designs identified using the surrogate and FEA models exhibit remarkably similar topological characteristics. For further comparison, the common types of conventional strut-based lattice structures are shown in Figure 6.

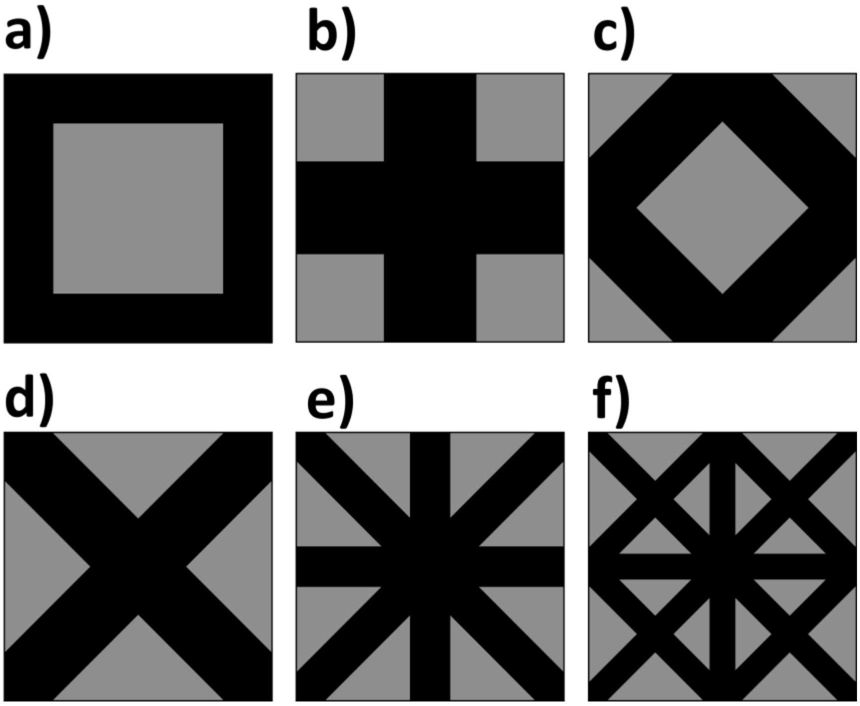

Figure 6 : Conventional strut-type lattice structures a) BC, b) BCC, c) DC, d) FCC, e) FBCC, f) FBCCDC.

The objective function values of these lattice structures are compared with the two optimum spinodal metamaterials as depicted in Figure 7.

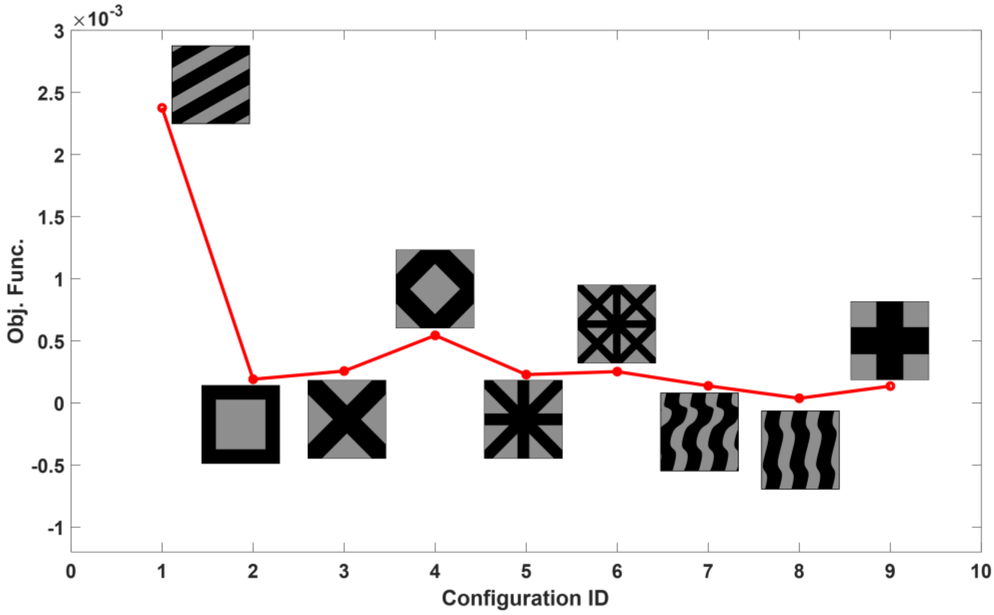

Figure 7 : Objective function comparison of surrogate-model-based and FEA-based optimum spinodoids with conventional strut-type lattices and the baseline spinodoid.

The improvements in the objective values relative to the baseline spinodal topology are listed in Table 2.

Table 2 : Energy fraction enhancements relative to the baseline model.

Structure Type	BC	BCC	DC	FCC	FBCC	FBCCDC	Surrogate Model	FEA
% Enhancement in E_f	92	94.3	77	89	90.4	89.4	94.2	98

As seen from Table 2, the surrogate-model-based optimum spinodal shape shows 94.2% improvement in terms of elemental energy fractions relative to the baseline model, and it shows better performance than most of the conventional strut-based lattices, while it shows similar performance with the BCC-type lattice. There is only a 3.8% difference between FEA and surrogate-model-based optimum spinodoids, which are in good agreement. The stress/strain field results in Figure 8 indicate that the optimum spinodal topology exhibits lower stress and strain distributions compared to traditional strut-based lattice geometries, in addition to a smoother distribution of stresses and strains as a result of their unique topology.

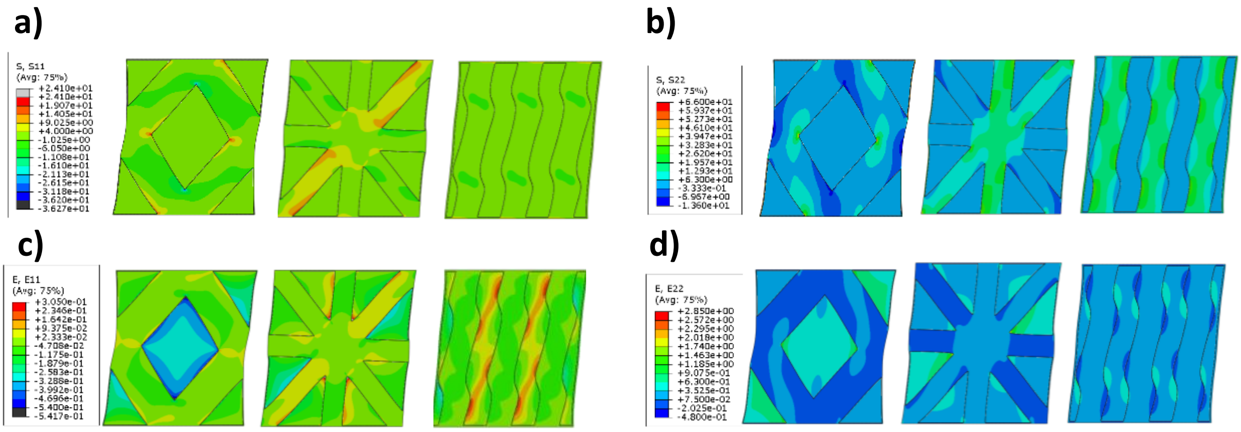

Figure 8: Stress and strain component distributions of optimum spinodoid, DC and FBCC (a) Stress along 1-1 direction (S_{11}), (b) Stress along 2-2 direction (S_{22}), (c) Strain along 1-1 direction (E_{11},) (d) Strain along 2-2 direction (E_{22}).

4.0 CONCLUSIONS

This study focuses on the development of an efficient deep-learning-based optimization framework to improve the mechanical performance of two-phase composite spinodal topologies. The specific conclusions of this data-driven design framework can be drawn as:

- The deep learning model was validated by comparing its optimum results with the optimization results utilizing the FEA simulations.

- The optimized spinodal topologies were compared with conventional strut-based lattices, whose geometries exhibit sharp corners that lead to increased stress and strain concentrations. The optimal spinodal structures exhibited up to a 21% relative improvement in mechanical performance compared to the strut-based lattices.

These findings are anticipated to support the potential utilization of spinodal metamaterials in broad engineering systems. These novel topologies can potentially replace conventional metamaterial designs in engineering structures used in military applications, enabled by advancements in additive manufacturing techniques.

ACKNOWLEDGEMENTS

The authors would like to acknowledge National Science Foundation (NSF) CAREER Award CMMI-2236947 and the Office of Naval Research (ONR) National Defense Education Program (NDEP) for Science, Technology, Engineering, and Mathematics (STEM) Education, Outreach, and Workforce Initiative Programs under Grant No. HQ0034231004 for the financial support.

REFERENCES

[1] Kumar, S., Tan, S., Zheng, L. and Kochmann, D.M. (2020). Inverse-designed spinodoid metamaterials. *npj Computational Materials*.

[2] Grant, C. P. (1993). Spinodal decomposition for the Cahn-Hilliard equation. *Communications in Partial Differential Equations*.

[3] Zheng, L., Kumar, S. and Kochmann, D.M. (2021). Data-driven topology optimization of spinodoid metamaterials with seamlessly tunable anisotropy. *Computer Methods in Applied Mechanics and Engineering*.

[4] Golnary, F., & Asghari, M. (2024). Data-driven analysis of spinodoid topologies: anisotropy, inverse design, and elasticity tensor distribution. *International Journal of Mechanics and Materials in Design*.

[5] Liu, S. and Acar, P. (2024). Generative Adversarial Networks for Inverse Design of Two-Dimensional Spinodoid Metamaterials. *AIAA Journal*.

[6] Jiexian, M. (2021). Im2mesh (2D image to triangular meshes) (https://www. mathworks. com/matlabcentral/fileexchange/71772-im2mesh-2d-image-to-triangular-meshes). *MATLAB Central File Exchange*.

[7] Al Abadi, H., Thai, H. T., Paton-Cole, V., & Patel, V. I. (2018). Elastic properties of 3D printed fibre-reinforced structures. *Composite Structures*.

[8] Torczon, V. (1997). On the convergence of pattern search algorithms. *SIAM Journal on Optimization*.